OPEN ACCESS
IOP Publishing
Classical and Quantum Gravity
Class. Quantum Grav. **42** (2025) 085017 (13pp)
https://doi.org/10.1088/1361-6382/adbcf3

Newtonian noise introduced by impellers in LIGO Voyager and Cosmic Explorer gravitational wave observatories

J A M Reis[1,*], E L Bonilla[2] and O D Aguiar[1]

[1] National Institute for Space Research, 2227-010 São José dos Campos, São Paulo, Brazil
[2] Stanford University, Stanford, CA 94305, United States of America

E-mail: juliedson.reis@inpe.br and odylio.aguiar@inpe.br

Received 2 September 2024; revised 9 November 2024
Accepted for publication 5 March 2025
Published 17 April 2025

Abstract

Third generation ground-based gravitational wave detectors are proposing the use of cryogenics. The low-temperature regime will require a cooling-down system capable of removing heat from test masses and maintaining its low temperature. The present study analyzes the Newtonian noise introduced by rotating impellers used in a cooling-down system with sub-cooled nitrogen circulating in a loop. In order to calculate this noise, a computational model was developed and the results were compared to the LIGO Voyager and Cosmic Explorer design sensitivity curves. For a system using two impellers having three blades each, the model shows that this Newtonian noise is always below the sensitivity curve if their distance to the test mass center is greater than 2.3 m for LIGO Voyager and 2.4 m for Cosmic Explorer. In addition, our calculations showed zero noise values for specific impeller's locations, depending on the blade number. This revealed a new region where it is possible to minimize the noise.

Keywords: cryogenic gravitational wave detector, LIGO Voyager, Cosmic Explorer, next-generation gravitational waves detector

* Author to whom any correspondence should be addressed.

Original Content from this work may be used under the terms of the Creative Commons Attribution 4.0 licence. Any further distribution of this work must maintain attribution to the author(s) and the title of the work, journal citation and DOI.

© 2025 The Author(s). Published by IOP Publishing Ltd

1. Introduction

In 2015, the LIGO detectors performed the first direct detection of gravitational waves [1], inaugurating the era of gravitational-wave astronomy. Since then, many more compact binary systems have been observed by the LIGO and Virgo collaborations [2–4]. To fully capitalize on the potential of the field, new technologies are constantly being developed in order to upgrade the current LIGO detectors, as well as supplementing the so-called 'third generation' gravitational-wave detectors, such as Cosmic Explorer [5], and the Einstein Telescope [6]. Many of the suggested upgrades will use heavier masses at cryogenic temperatures to reduce some fundamental noises.

In addition to the low-temperature regime, silicon-made test masses will be used for LIGO Voyager [7] and possibly for Cosmic Explorer [6]. Particularly, this material presents a zero thermal expansion coefficient around 123 K [8] and, operating at this temperature, it is possible to suppress the thermoelastic noise [9].

Considering the LIGO Voyager design, about 10 W of power needs to be extracted from the test mass to maintain its temperature of 123 K [10]. The high vacuum inside the chambers makes convection negligible. Furthermore, metallic links to conduct heat from the test masses could introduce noise by the vibration modes [11, 12]. Nevertheless, it is possible to remove the required heat by radiation. For this purpose, a closed-loop pipeline in which a sub-cooled (65–77 K) liquid nitrogen (LN2) is circulating can be used. However, this system can introduce Newtonian noise due to bubble formation, which was addressed by Bonilla *et al* [13].

On the other hand, in order to circulate a sub-cooled liquid nitrogen in a closed-loop pipeline, a novel pumping device is required. We propose the use of magnetically driven rotating impellers to create the LN2 flux. Because this mechanism will also generate Newtonian noise, we present a model for the gravitational interaction between these impellers and the test mass, and estimate the noise it produces to evaluate the viability of this system.

2. Methods

In order to estimate the Newtonian noise introduced by the impellers, one needs to calculate the gravitational interaction between each impeller and the test mass. Consider n_p impellers of n_b blades. In a first approach, each blade was modeled as a point mass circulating a center (the impeller center) at a frequency f (in Hz). A vector $\vec{r}$ points from the center of mass of the test mass to each point of mass (blade), and it makes an angle θ with the symmetry axis of the cylinder.

The gravitational force exerted on an uniform cylinder by a point mass was investigated by Lockerbie *et al* [14]. Similarly to Bonilla *et al* [13]. The axial acceleration per unit mass can be expanded in terms of the the ratio of cylinder length l, and the distance of the point mass to the center of the cylinder r as follows:

$$\alpha(r,\theta) = G\cdot\sum_{n=0}^{\infty}\left[\frac{P_{2n+1}(\cos\theta)}{r^2}\left(\frac{l}{2r}\right)^{2n}\sum_{k=0}^{n}\binom{2n+1}{2k}\frac{P_{2k}(0)}{k+1}\left(\frac{2b}{l}\right)^{2k}\right], \tag{1}$$

where b is the cylynder radius, and θ is the azimuthal angle, as defined in figure 1. In addition, $P_k(x)$ represents the kth Legendre polynomial.

Equation (1) gives the axial acceleration $\alpha(r,\theta)$ due to each blade (point mass) at a given moment in time. The sum of the contributions of all blades gives the total axial acceleration for one specific impeller, and the sum of all impellers' contributions results in the total axial

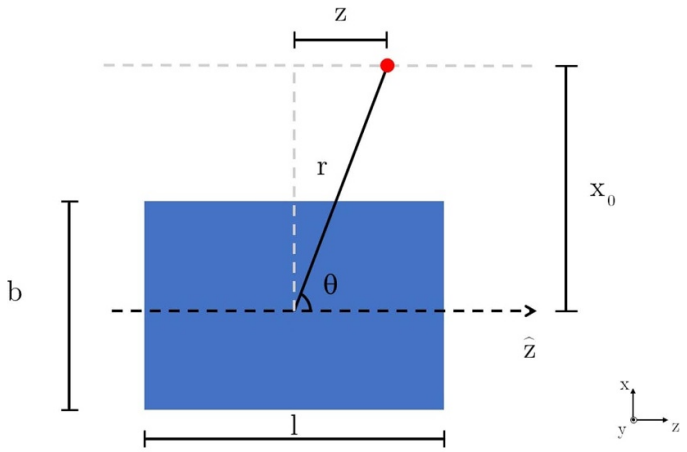

Figure 1. Representation of the test mass side view, with the coordinate system chosen for the calculations. Note that the axis in which the we put the impellers' centers is parallel to the test mass symmetry axis (z axis), and these two are separated by a distance x_0.

acceleration. Furthermore, the blades rotate with frequency f, i.e. their position is a function of time, as is the total axial acceleration as well. Therefore, the equation can be seen as a time series through the dependence of θ on time.

For this model, we are considering a pipeline system that includes a serpentine around the test mass low temperature shield, and a liquid nitrogen flux produced by two impellers, one at the input and one at the output. In addition, the vector normal to the impeller's plane is pointed towards the test mass symmetry axis. Furthermore, the axis formed by the impellers' centers is parallel to the same test mass symmetry axis, and these two are separated by a distance x_0. Considering $l/2$ the half length of the test mass and the origin of the coordinates at the cylinder center of mass, as in (1), the impellers' centers are located at the points $(x_0, 0, l/2)$ and $(x_0, 0, -l/2)$.

In figure 1, one can see a representation of the coordinate system chosen for the calculations. The point mass is represented by a dot and the test mass, side viewed, by a rectangle. In general, the impellers' centers are at the points $(x_0, 0, z)$.

In figure 2, it is given another view for the system, using a general position for the impeller's center (small dot). Its position is at the point $(x_0, 0, z)$. The blades, considered point masses, are represented by three dots.

For a given configuration of n_p, n_b, x_0, and f, the model can generate a total axial acceleration time series. Since we have it in the Fourier domain, using common algorithms of Fourier Transform, it is integrated twice, resulting in the power spectral density (PSD) of displacement. Finally, taking the square root of the PSD, it calculates the amplitude spectral density (ASD) of the displacement in units of $\mathrm{m}/\sqrt{\mathrm{Hz}}$. Therefore, we compare it to LIGO Voyager and Cosmic Explorer designed curves for ASD of displacement.

All impellers are in phase and have the same rotational frequency f, which is the worst case for producing Newtonian noise. Nevertheless, an even number of impeller blades should, in principle, minimize the noise due to the symmetry of the blade arrangement. The effect of one impeller blade on the test mass is roughly canceled out by the effect of the opposite one. This

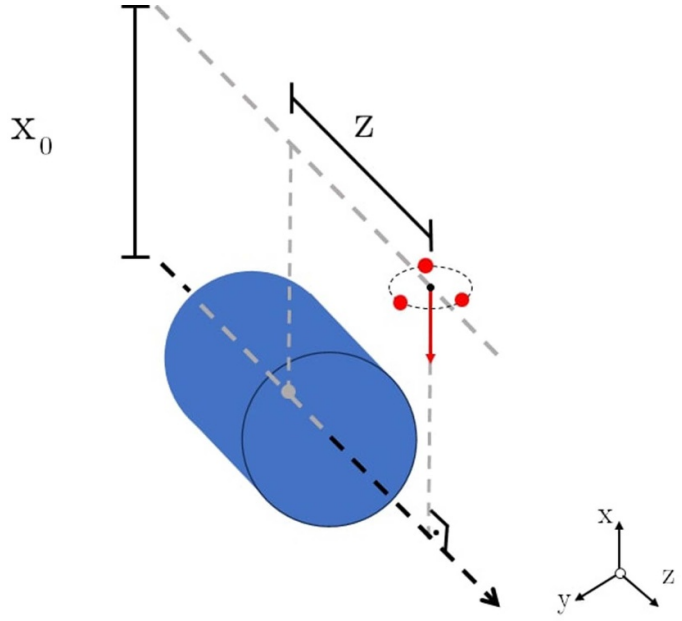

Figure 2. Representation of the coordinate system chosen for the calculations. The impellers blades are represented by dots. The vector normal to the impeller's plane is pointed towards the test mass symmetry axis.

cancellation is not perfect, because the distances to the test mass, considering opposite blades in the same impeller, are not exactly the same.

It is important to note that LIGO Voyager and Cosmic Explorer do not have the same test mass design. LIGO Voyager uses a length of $l_v = 550$ mm and diameter $d_v = 450$ mm [7]. In the case of the Cosmic Explorer, because the dimensions of its test mass have not yet been fully defined, we used two sets of parameters (length and diameter): one is $l_c = 644$ mm and $d_c = 526$ mm, the other is $l_c = 880$ mm and $d_c = 450$ mm. For our results, we considered $x_0 \geqslant 1.0$ m, an impeller mass of $m = 100$ g, and an impeller radius of $\delta = 8$ cm.

3. Results and discussions

3.1. Analysis for different configurations

In order to compare the different results for distinct configurations, let us consider first $n_\mathrm{p} = 2$. Table 1 shows the comparison between the Newtonian noise calculated for impellers of 3 and 5 blades for all studied configurations. As it is expected, the larger the distance x_0 the less noise. Additionally, the noise caused by impellers of $n_\mathrm{b} = 5$ is lower than the one caused by impellers of $n_\mathrm{b} = 3$. This is because adding more blades means a less anisotropic distribution of mass. Consequently, a large number of blades implies less Newtonian noise.

For the Voyager case shown in figure 3, the noise produced by 3-bladed impellers can be 10^5 bigger than the 5-bladed one, depending on the distance x_0. In the Cosmic Explorer case, as seen in table 1, there are similar ratios in noise peaks, ranging from 10^3 to 10^5 depending on x_0. For $x_0 \geqslant 2$ m, the peaks of 5-blade calculations are below $\approx 10^{-25}$ m $\sqrt{\mathrm{Hz}}^{-1}$.

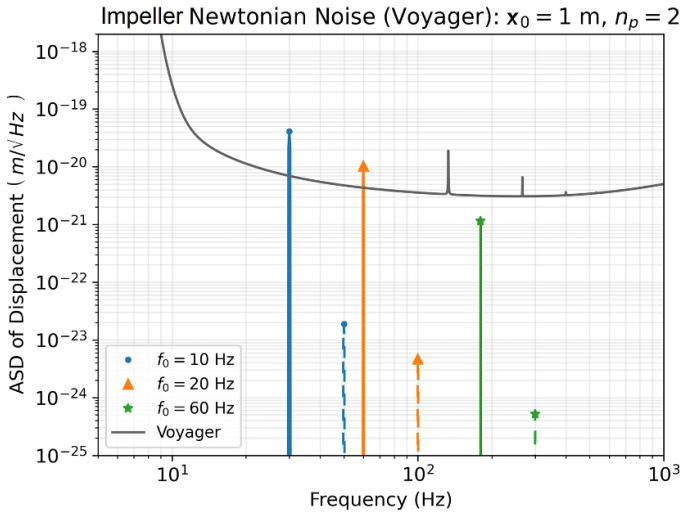

Figure 3. Newtonian noise for Voyager, $x_0 = 1$ m and different number of blades. The chosen impeller rotation frequencies are $f_0 = 10, 20,$ and 60 Hz. Solid lines show the Newtonian Noise for $n_\mathrm{b} = 3$, while dashed lines show the same noise but using $n_\mathrm{b} = 5$. Circle, triangle and star represent $f = 10$ Hz, $f = 20$ Hz, $f = 60$ Hz peaks, respectively.

Also in table 1, we compare the maxima noise values calculated. One can note that the ratio between Voyager and CE is dependent on the distance x_0 and the number of blades n_b, which means 3-bladed impellers generate more noise.

Finally, focusing on the frequencies, it can be noted that different impeller rotation frequencies f_0 will result in a peak noise at $f_n = f_0 \cdot n_\mathrm{p}$. Assuming that the noise frequency is stable, we highlight that it is possible to use a notch filter to attenuate it. In the same way, one can design its frequency to match the power line noise or one of the wire suspension lines, since they are usually removed from the spectra. If the noise coupling is linear and not affected by other coupling mechanisms, it is also possible to try to cancel it, since the value is well known.

Next, we will discuss a safe distance that we can choose in order to have the impellers' noise level bellow the sensitivity curve. Therefore, we defined a maximum threshold of $1/10$ times the detector's sensitivity curve. Figures 4–6 shows the sensitivity curve for Voyager, CE1 and CE2, respectively. Also, one can note noise maxima for different frequencies f_0 and distances y_0. We used $f = 1, 2, 3, 4, 5, 6, 7, 8, 9, 10, 20, 60,$ and 100 (Hz). Additionaly, let us consider $n_\mathrm{b} = 3$, since this noise is higher than that produced by impellers with $n_\mathrm{b} = 5$ (see figure 3).

For LIGO Voyager configuration, our model shows that the noise peak will lie below threshold, for all frequencies, if $x_0 \geqslant 2.3$ m (figure 4). Cosmic Explorer results were also calculated. For the first test mass dimensions ($l_c = 644$ mm and $d_c = 526$ mm), all noise peaks are below threshold for all frequencies if $x_0 \geqslant 2.4$ m (figure 5). For the other test mass dimensions ($l_c = 880$ mm and $d_c = 450$ mm), all noise maxima are smaller than the sensitivity curve if $x_0 \geqslant 2.6$ m (figure 6). In addition, if $x_0 \geqslant 3$ m the noise peaks will lie below threshold for all three configuration. Also, impellers at distances $x_0 \geqslant 1$ m produce noise peaks below the threshold for analysed designs if $n_\mathrm{b} = 5$. These results are summarized in table 2. The impellers are responsible for generating flux pushing the liquid forward. In particular, a lower pressure region is created behind each blade. Depending on its angular velocity and the flux

Table 1. Maxima of the ASD of displacement Newtonian noise values calculated for LIGO Voyager and Cosmic Explorer (CE), using $l_c = 644\,\text{mm}$ and $d_c = 526\,\text{mm}$, with the ratio between Voyager and CE results.

x_0 (m)	n_p	n_b	f_0 (Hz)	Voyager ASD ($\text{m}\sqrt{\text{Hz}}^{-1}$)	CE ASD ($\text{m}\sqrt{\text{Hz}}^{-1}$)	Ratio
1	2	3	10	$4.141 \cdot 10^{-20}$	$4.360 \cdot 10^{-20}$	0.950
1	2	3	20	$1.035 \cdot 10^{-20}$	$1.090 \cdot 10^{-20}$	0.950
1	2	3	60	$1.150 \cdot 10^{-21}$	$1.211 \cdot 10^{-21}$	0.950
1	2	5	10	$1.874 \cdot 10^{-23}$	$2.486 \cdot 10^{-23}$	0.754
1	2	5	20	$4.685 \cdot 10^{-24}$	$6.214 \cdot 10^{-24}$	0.754
1	2	5	60	$5.206 \cdot 10^{-25}$	$6.905 \cdot 10^{-25}$	0.754
2	2	3	10	$5.073 \cdot 10^{-22}$	$6.141 \cdot 10^{-22}$	0.826
2	2	3	20	$1.268 \cdot 10^{-22}$	$1.535 \cdot 10^{-22}$	0.826
2	2	3	60	$1.409 \cdot 10^{-23}$	$1.706 \cdot 10^{-23}$	0.826
2	2	5	10	$1.492 \cdot 10^{-26}$	$2.346 \cdot 10^{-26}$	0.636
2	2	5	20	$3.730 \cdot 10^{-27}$	$5.865 \cdot 10^{-27}$	0.636
2	2	5	60	$4.145 \cdot 10^{-28}$	$6.517 \cdot 10^{-28}$	0.636
3	2	3	10	$3.213 \cdot 10^{-23}$	$3.978 \cdot 10^{-23}$	0.808
3	2	3	20	$8.032 \cdot 10^{-24}$	$9.945 \cdot 10^{-24}$	0.808
3	2	3	60	$8.925 \cdot 10^{-25}$	$1.105 \cdot 10^{-24}$	0.808
3	2	5	10	$1.832 \cdot 10^{-28}$	$2.923 \cdot 10^{-28}$	0.627
3	2	5	20	$4.581 \cdot 10^{-29}$	$7.308 \cdot 10^{-29}$	0.627
3	2	5	60	$5.090 \cdot 10^{-30}$	$8.120 \cdot 10^{-30}$	0.627

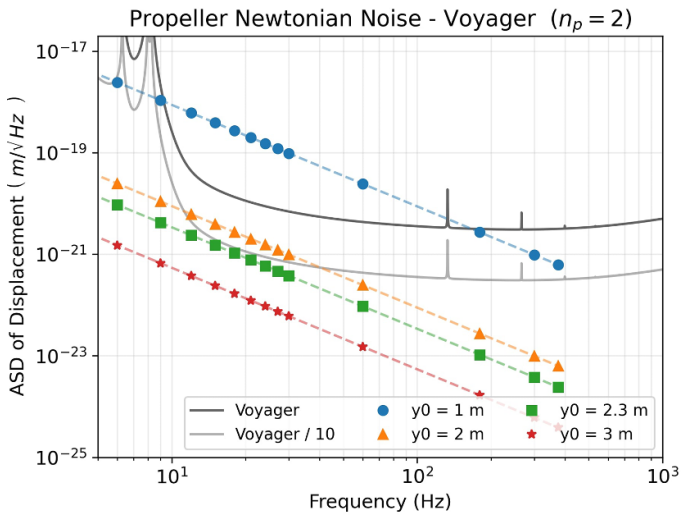

Figure 4. Newtonian noise peaks for different impeller rotation frequencies in the LIGO Voyager configuration.

rate, the LN2 boiling point can be lowered enough to form bubbles, which can merge into a single one, behind each blade. These attached bubbles will reduce the Newtonian noise caused by the impellers. However, this possibility needs more investigation.

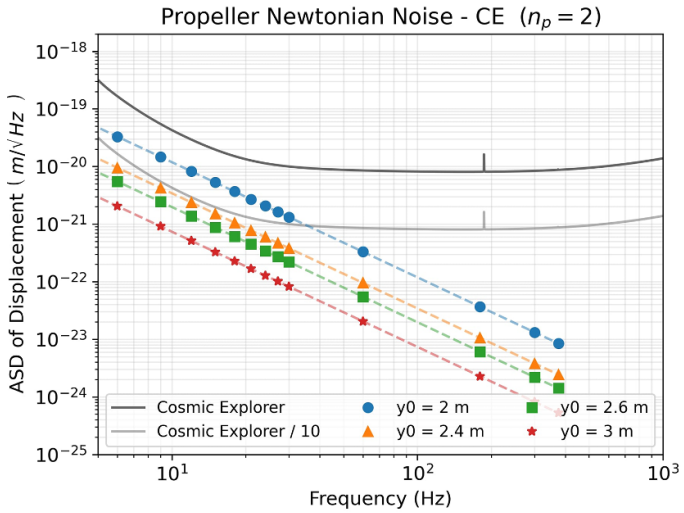

Figure 5. Newtonian noise peaks for different impeller rotation frequencies in the Cosmic Explorer configuration, using $l_c = 644\,\text{mm}$, $d_c = 526\,\text{mm}$.

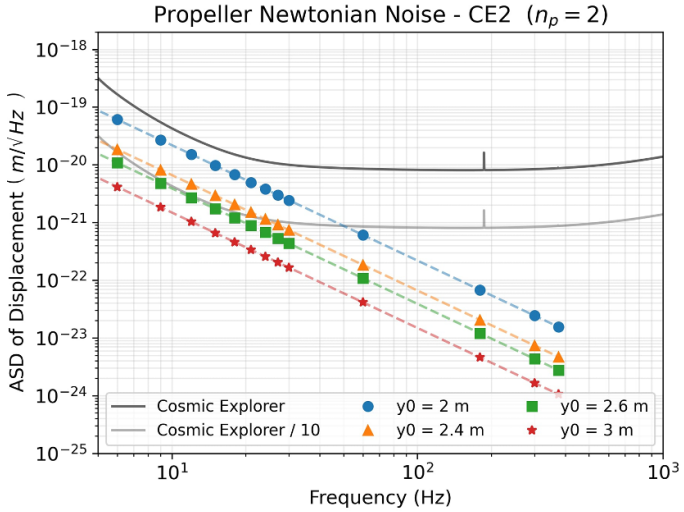

Figure 6. Newtonian noise peaks for different impeller rotation frequencies in the Cosmic Explorer configuration, using $l_c = 800\,\text{mm}$, $d_c = 450\,\text{mm}$.

3.2. Newtonian noise zero

The impeller's centers are located at the points $(x_0, 0, z)$. Varying the z coordinate, we calculated the noise peak for different impellers' center positions. The results show a zero noise for a specific θ_0 angle, which implies a specific z coordinate, depending on the number of blades n_b. Note that θ_0 is the angle formed by the vector pointing from the origin to the impeller's center and the z axis.

Table 2. Minimum x_0 (m) in which all peaks are below the sensitivity curve calculated for LIGO Voyager and Cosmic Explorer.

Detector	l (mm)	d (mm)	n_b	x_0 (m)
LIGO Voyager	550	450	3	1.35
			5	1.0
Cosmic Explorer	644	526	3	1.4
			5	1.0
Cosmic Explorer	800	450	3	1.5
			5	1.0

On figure 7, one can see the plot for the ASD of displacement calculated for one impeller with 3 blades, $x_0 = 1$ m, and $f = 20$ Hz. Varying the z coordinate, the model resulted in a zero value around $z \approx 0.8918$ m.

The cancellation of the Newtonian noise can be understood by expanding (1) to first relevant order in (δ/r_0), where δ is the impeller radius, and r_0 is the distance between the center of the impeller and the center of the test mass. If we only expand the monopole term for the axial acceleration for n_b blades, the lowest order α_0 is given by (see appendix for more details):

$$\alpha_0 = \frac{G}{r_0^2}\left(\frac{\cos(\theta_0)}{2}\right)^{n_\mathrm{b}-1}\frac{(2n_\mathrm{b}+1)!!}{(n_\mathrm{b}-1)!}\left[\cos^2(\theta_0) - \frac{n_\mathrm{b}}{2n_\mathrm{b}+1}\right]\left(\frac{\delta}{r_0}\right)^{n_\mathrm{b}}\cos(n_\mathrm{b}\beta(t)), \tag{2}$$

where θ_0 is the azimuth angle of the center of the impeller, and $\beta(t)$ represents the time-dependent angular motion of the impeller. Therefore, the monopole contribution to impeller Newtonian noise from this equation becomes zero at:

$$\theta_0 = \arccos\left[\left(\frac{n_\mathrm{b}}{2n_\mathrm{b}+1}\right)^{1/2}\right]. \tag{3}$$

Equation (3) gives an approximation for the z coordinate at the zero Newtonian noise. For one impeller of 3 blades, as shown in figure 7, we have $\theta_0 \approx 49.1^o$. This corresponds to $z \approx 0.8660$.

This expansion helps explain the nature of the Newtonian noise zero: the gravitational effect of a rotating blade varies depending on its proximity to the center of the cylinder. As the blade moves closer to the center, the gravitational pull strengthens. However, this proximity also causes the mass to deviate further from the symmetry axis of the cylinder in terms of azimuthal angle, thereby weakening the axial projection of the gravitational force. These two opposing effects are of comparable magnitude and can nullify each other at a specific angle θ_0, as calculated.

In a realistic design for the cryogenic system, we can select the impeller position and orientation so as to minimize the impact of their Newtonian coupling to the test mass.

4. Conclusion

We studied the Newtonian noise generated by impellers used in a closed-loop pipeline cooling-down system for cryogenic detectors. For this purpose, a model was developed in order to

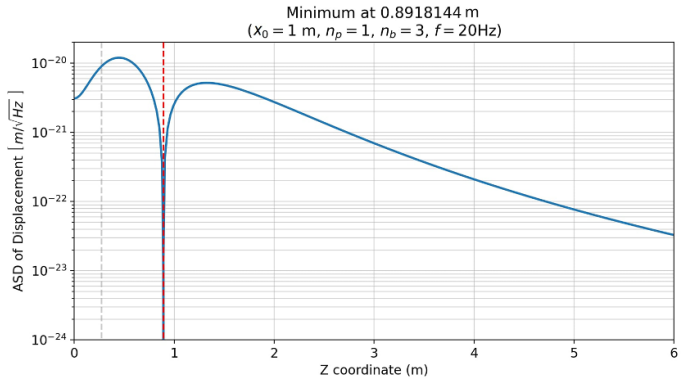

Figure 7. Noise peaks for different z coordinates, using the Voyager design configuration, $x_0 = 1.0\,\mathrm{m}$, $n_\mathrm{p} = 3$, and $f = 20\,\mathrm{Hz}$. The zero is located at $z \approx 0.8918$ m. The red dashed line denotes the minimum position, while the gray dashed line represents the test mass half-length. This profile is the same for negative z coordinates.

estimate the gravitational interaction between the impeller and the test mass. The model was then applied to the LIGO Voyager and Cosmic Explorer test masses.

From the results, this study sheds some light on the design choices. The minimum distance from the test mass to the impellers in which the Newtonian noise is lower than the sensitivity curve will depend on the number of blades. The results for $n_\mathrm{b} = 3$ are, in LIGO Voyager case, $x_0 \geqslant 1.35\,\mathrm{m}$. For Cosmic Explorer, we analyzed two different test mass possibilities and, for the minimum distance x_0 can be 1.4 m or 1.5 m. However, considering $n_\mathrm{b} = 5$, the peaks are below the sensitivity curve if $x_0 \geqslant 1.0\,\mathrm{m}$ for all considered detectors designs.

Furthermore, our model revealed another possibility for the impeller's position choice: the combination of blades position and angle produces a noise zero for specific positions in our coordinate system. In addition, there is a region around the minimum position which results in lower noise levels and can be used to allocate more than one impeller, if needed.

Therefore, by ensuring that the distance criterion is met, the formation of bubbles on the pipeline walls [13] becomes a greater concern than impeller Newtonian noise for LIGO Voyager and Cosmic Explorer.

The model has certain limitations, as one can note. Firstly, it treats the blades as point masses, which can be improved by representing each blade as several equal-mass points and calculating their contributions to the total axial acceleration. Moreover, the Newtonian noise results for the case of the Cosmic Explorer need to be reviewed if its test masses are produced with other dimensions than the ones we assumed in this work.

Data availability statement

No new data were created or analysed in this study.

Acknowledgments

The authors would like to thank Brazilian Ministry of Science, Technology and Inovation, and the Brazilian Space Agency (AEB), which supported the present work under PO 20VB.0009. Support from the Conselho Nacional de Desenvolvimento Cientifíco e Tecnológico (CNPq)

is also acknowledged under Grant No. 310087/2021-0. This study was financed in part by X. *Coordenação de Aperfeiçoamento de Pessoal de Nível Superior*—Brasil (CAPES)—Finance Code 001. This material is based upon work supported by NSF's LIGO Laboratory which is a major facility fully funded by the National Science Foundation.

Appendix. Newtonian noise zero detailed calculations

A.1. Introduction

In our model, we consider an impeller in which blades of n_b point masses are symmetrically spaced around a center location denoted by $\vec{r}_0 = r_0\hat{u}_r$. The cylindrical test mass of radius b and half length $l/2$. The radius of the impeller is denoted by δ. Following figure 2, we can write the position of a blade relative to the center of the impeller as:

$$\vec{\delta}_k = \delta\left[-\cos\left(\beta_k\right)\hat{z} + \sin\left(\beta_k\right)\hat{y}\right]. \tag{A.1}$$

The n_b angles $\beta_k = \beta(t) + 2\pi k/n_\mathrm{b}$, $k = 0, 1, \cdots, n_\mathrm{b} - 1$ are the angles of the equidistant point masses. In this definition, $\beta(t)$ is the common angle that describes the rotation of the impeller. The choice of measuring angles using the negative z axis is arbitrary and does not affect the results of our calculations, but we adopt it because it simplifies calculations down the line.

We can analyze the axial acceleration made by the kth point mass of the impeller by calculating the time dependent position of the point mass:

$$\begin{aligned}\vec{r}_k &= \vec{r}_0 + \vec{\delta}\\ &= \left[r_0\cos\left(\theta_0\right) - \delta\cos\left(\beta_k\right)\right]\hat{z} + r_0\sin\left(\theta_0\right)\hat{x} + \delta\sin\left(\beta_k\right)\hat{y}.\end{aligned} \tag{A.2}$$

Its amplitude:

$$\begin{aligned}r_k &= \sqrt{\left(\vec{r}_0 + \vec{\delta}\right)\cdot\left(\vec{r}_0 + \vec{\delta}\right)}\\ &= \sqrt{r_0^2 + \delta^2 - 2r_0\delta\cos\left(\theta_0\right)\cos\left(\beta_k\right)},\end{aligned} \tag{A.3}$$

and the cosine to the azimuth:

$$\begin{aligned}\cos\left(\theta_k\right) &= \frac{r_0\cos\left(\theta_0\right) - \delta\cos\left(\beta_k\right)}{r_k}\\ &= \left[r_0\cos\left(\theta_0\right) - \delta\cos\left(\beta_k\right)\right]\left[r_0^2 + \delta^2 - 2r_0\delta\cos\left(\theta_0\right)\cos\left(\beta_k\right)\right]^{-1/2}.\end{aligned} \tag{A.4}$$

Plugging these definitions for each blade into the (1), one can estimate the impeller's Newtonian noise per unit mass.

A.2. Relevant approximations

In the following, we attempt to approximate the Newtonian noise to the first relevant order in δ/r_0. First, we expand $1/r_k^n$ by using (A.3), and factor out the term going as $r_0^2 + \delta^2$:

$$\left(\frac{1}{r_k}\right)^n = \left(r_0^2 + \delta^2\right)^{-n/2}\left[1 - \frac{2r_0\delta\cos\left(\beta_k\right)\cos\left(\theta_0\right)}{r_0^2 + \delta^2}\right]^{-n/2}. \tag{A.5}$$

Next, we separate the higher-mode contributions of $\cos(\beta_k)$ by using the generalized binomial expansion:

$$(1-x)^{-s} = \sum_{m=0}^{\infty} \binom{s+m-1}{m} x^m, \tag{A.6}$$

where the generalized binomial coefficient is evaluated to be $\binom{n}{m} = n(n-1)(n-m+1)/m!$. Expanding A.5 by identifying x in (A.6) with the $\cos(\beta_k)$ term yields:

$$\left(\frac{1}{r_k}\right)^n = \frac{1}{r_0^n}\left[1+(\delta/r_0)^2\right]^{-n/2} \times \sum_{m=0}^{\infty} \binom{m+n/2-1}{m} \left[\frac{2\cos(\theta_0)\,(\delta/r_0)}{1+(\delta/r_0)^2}\right]^m \cos^m(\beta_k). \tag{A.7}$$

We observe that the leading term accompanying $\cos^m(\beta_k)$ is proportional to $(\delta/r_0)^m$. This is relevant because the symmetry of the impeller implies that only harmonics of the number of masses n_b will ultimately contribute to Newtonian noise, therefore resulting on suppression of the noise with increasing number of impeller blades. We can prove this fact by looking at the Fourier expansions for the powers of $\cos(x)$:

$$\cos^m(x) = \frac{1}{2^{m-1}} \sum_{k=\lfloor (m+1)/2 \rfloor}^{m} \binom{m}{k} \cos\left[(2k-m)x\right] \tag{A.8}$$

for odd values of m, and

$$\cos^m(x) = \frac{1}{2^{m-1}} \sum_{k=(m/2)+1}^{m} \binom{m}{k} \cos\left[(2k-m)x\right] + \frac{1}{2^m}\binom{m}{m/2}$$

for even values of m.

If we add the contribution of all the masses of an impeller, we note that only harmonics of the number of impellers n_b do not cancel each other out, since

$$\begin{aligned}\sum_{k=0}^{n_\mathrm{b}-1} \cos\left[n\left(\beta + 2\pi k/n_\mathrm{b}\right)\right] &= \mathrm{Re}\left\{\exp(\mathrm{i}n\beta) \sum_{k=0}^{n_\mathrm{b}-1} \left[\exp(2\pi \mathrm{i}n/n_\mathrm{b})\right]^k\right\} \\ &= \begin{cases} n_\mathrm{b}\cos(n\beta) & \text{for } n/n_\mathrm{b} \in \mathrm{Z}, \\ 0 & \text{for } n/n_\mathrm{b} \notin \mathrm{Z}. \end{cases}\end{aligned} \tag{A.9}$$

Therefore, the contributions from an impeller of n_b masses will go as a sum of $\cos(n_\mathrm{b}\beta), \cos(2n_\mathrm{b}\beta), \ldots$ In general, an impeller of n_b point masses will have its lowest order nonzero contribution be proportional to $(\delta/r_0)^{n_\mathrm{b}}\cos(n_\mathrm{b}\beta)$, coming from the Fourier expansion of $\cos^{n_\mathrm{b}}(\beta_k)$.

A.3. Expansion of the monopole term

Expanding the entire summation in (1) in a general way is very challenging. However, it is possible to learn more about the nature of the Newtonian coupling by looking at an expansion of the monopole term to the first relevant order on (δ/r_0).

$$
\begin{aligned}
G\cos\left(\theta_k\right) r_k^{-2} &= G r_0 \left[\cos\left(\theta_0\right) - \delta\cos\left(\beta_k\right)/r_0\right] r_k^{-3} \\
&= G\left[\cos\left(\theta_0\right) - \delta\cos\left(\beta_k\right)/r_0\right]\left\{r_0^2\left[1+\left(\delta/r_0\right)^2\right]^{3/2}\right\} \\
&\quad\times\sum_{m=0}^{\infty}\binom{m+1/2}{m}\left[\frac{2\cos\left(\theta_0\right)\left(\delta/r_0\right)}{1+\left(\delta/r_0\right)^2}\right]^m\cos^m\left(\beta_k\right). \qquad \text{(A.10)}
\end{aligned}
$$

Note that the term $[\cos(\theta_0) - (\delta/r_0)\cos(\beta_k)]$ selects adjacent terms in the expansion. This term represents the competing effects of an impeller blade approaching the center of mass of the cylinder (which increases the axial gravitational force) and the one moving from the axis of symmetry of the cylinder (which decreases the axial gravitational force).

As discussed previously, when we add the contribution from all the n_b impellers, the first term of the expansion that does not cancel goes as $\cos^{n_\mathrm{b}}(\beta_k)$. To lowest order in δ/r_0, the monopole contribution of the kth impeller mass to the axial acceleration is given by:

$$
\frac{G}{r_0^2}\left[\binom{n_\mathrm{b}+1/2}{n_\mathrm{b}}2^{n_\mathrm{b}}\cos^{n_\mathrm{b}+1}\left(\theta_0\right) - \binom{n_\mathrm{b}-1/2}{n_\mathrm{b}-1}2^{n_\mathrm{b}-1}\cos^{n_\mathrm{b}-1}\left(\theta_0\right)\right]\left(\frac{\delta}{r_0}\right)^{n_\mathrm{b}}\cos^{n_\mathrm{b}}\left(\beta_k\right). \qquad \text{(A.11)}
$$

We can simplify (A.11) with the identity:

$$
\binom{n_\mathrm{b}+1/2}{n_\mathrm{b}} = \frac{(2n_\mathrm{b}+1)!!}{2^{n_\mathrm{b}}n_\mathrm{b}!}. \qquad \text{(A.12)}
$$

After adding all the impeller blades:

$$
\frac{n_\mathrm{b}\cdot G}{r_0^2}\left[\frac{\cos\left(\theta_0\right)}{2}\right]^{n_\mathrm{b}-1}\left[\frac{(2n_\mathrm{b}+1)!!}{n_\mathrm{b}!}\cos^2\left(\theta_0\right) - \frac{(2n_\mathrm{b}-1)!!}{(n_\mathrm{b}-1)!}\right]\left(\frac{\delta}{r_0}\right)^{n_\mathrm{b}}\cos\left(n_\mathrm{b}\beta\right). \qquad \text{(A.13)}
$$

Finally, this first order approximation to the monopole term, (A.13) becomes zero at $\theta_0 = \arccos\left[\left(n_\mathrm{b}/2n_\mathrm{b}+1\right)^{-1/2}\right]$.

ORCID iDs

J A M Reis https://orcid.org/0000-0001-7372-1827
E L Bonilla https://orcid.org/0000-0002-6284-9769
O D Aguiar https://orcid.org/0000-0002-2139-4390

References

[1] Abbott B P *et al* (LIGO Scientific Collaboration) 2016 *Phys. Rev. Lett.* **116** 061102
[2] Abbott B P *et al* 2019 *Phys. Rev.* X **9** 031040
[3] Abbott B P *et al* (LIGO Scientific Collaboration and Virgo Collaboration) 2021 *Phys. Rev.* X **11** 021053
[4] Abbott B P *et al* (LIGO Scientific Collaboration, Virgo Collaboration and KAGRA Collaboration) 2023 *Phys. Rev.* X **13** 041039
[5] Hall E D 2022 *Galaxies* **10** 90

[6] Maggiore M *et al* 2020 *J. Cosmol. Astropart. Phys.* JCAP03(2020)050
[7] LSC 2021 Instrument science whitepaper 2021 *Technical Report* (LIGO Scientific Collaboration) (available at: www.ligo.org/)
[8] Kim D S, Hellman O, Herriman J, Smith H L, Lin J Y Y, Shulumba N, Niedziela J L, Li C W, Abernathy D L and Fultz B 2018 *Proc. Natl Acad. Sci. USA* **115** 1992–7
[9] Adhikari R X *et al* 2020 *Class. Quantum Grav.* **37** 165003
[10] Constancio M Jr, Adhikari R X, Aguiar O, Arai K, Markowitz A, Okada M and Wipf C C 2020 *Int. J. Heat Mass Transfer* **157** 119873
[11] Bajpai R, Tomaru T, Kimura N, Ushiba T, Yamamoto K, Suzuki T and Honda T 2022 *Class. Quantum Grav.* **39** 165004
[12] Yamada T, Tomaru T, Suzuki T, Ushiba T, Kimura N, Takada S, Inoue Y and Kajita T 2021 *Cryogenics* **116** 103280
[13] Bonilla E, Shapiro B, Lantz B, Aguiar O D and Constancio M 2021 *Phys. Rev.* D **104** 122005
[14] Lockerbie N A, Xu X and Veryaskin A V 1996 *Class. Quantum Grav.* **13** 2041